Ceramics International **22** (1996) 397–401

0272-8842(95)00122-0
0272-8842/96 $15.00 + .00

Thermal Crack Initiation Mechanisms on the Surface of Functionally Graded Ceramic Thermal Barrier Coatings

K. Kokini, Y. R. Takeuchi & B. D. Choules

Purdue University, School of Mechanical Engineering, West Lafayette, IN 47907-1288, USA

(Received 7 July 1995; accepted 29 August 1995)

Abstract: The surface crack initiation mechanism in a multilayer zirconia/metal coating on a steel substrate was determined to be tensile stresses which are generated by cooling after relaxation of the compressive stresses at high temperature. This crack initiation criterion is utilized to study the architectural design of a functionally graded coating. © 1996 Elsevier Science Limited and Techna S.r.l.

1 INTRODUCTION

The next generation of heat engines will have to sustain increasingly larger temperatures. In order to achieve such high temperature environments the metallic parts will have to be protected. Ceramic coatings offer an excellent way of insulating and protecting metallic components. However, the thermal cyclic loads applied to these materials result in their cracking, delamination and spalling. In order to prevent or delay such failures, the mechanisms which cause initiation and propagation of the cracks need to be understood. Several studies have considered the time to spalling under different thermal loading conditions.[1–3] In this article, the research of the present authors related to determine the initiation of the first surface crack under controlled transient thermal loads is reviewed.

2 SURFACE CRACK INITIATION MECHANISM

The specimens shown in Fig. 1 were used for this research. They consist of a steel beam with a plasma-sprayed multilayer coating. The layers are graded such that the steel is coated with a bond coat (CoCrAlY), then 40% zirconia/60% bond coat, followed by 85% zirconia/65% bond coat and finally 100% zirconia.

The experimental set-up is shown in Fig. 2. It consists of two high-intensity focused infrared lamps which project a line heat flux at the centre of the surface of the specimen. The bottom of the substrate is cooled via contact with a water cooled plate. The effect of subjecting the specimen to such heating is shown in Fig. 3, which defines the quantitative boundary conditions for the transient heat transfer into the specimen.

The experiment performed consisted of heating the surface of the specimen until steady-state, leave it at this temperature distribution for two hours and allowing it to cool to room temperature. The temperature distribution which results from heating is shown in Fig. 4. In all cases it was determined that a surface crack formed underneath the lamp, in the region where the heat flux was focused.

In order to determine the reasons for such crack initiation the experiment was modelled using the finite element method. The details of this calculation have been presented elsewhere and will not be repeated here.[4,5] The stress distribution was calculated in four consecutive steps which consisted of: (1) calculating the residual stresses caused by cooling from a uniform steady-state temperature of 590°C; (2) determining the stresses caused by the steady-state temperature; (3) letting the stresses relax for 2 h based on an assumed power law relationship shown in eqn (1) below; (4) calculating the stresses caused by uniform cooling to

room temperature which follows the stress relaxation.

The power-law model used for stress relaxation was:

$$\dot{\epsilon} = A\sigma^n e^{-\frac{\Delta H}{RT}} \quad (1)$$

where σ = Von Mises equivalent stress, ΔH = activation energy (4.605×10^{19}/kJ/atm), R = universal gas constant (1.38×10^{-23} kJ/atmK), A = experimental constant (1.89×10^{-6}(N/m^2)$^{-n}$ (l/s)), n = experimental constant (1.59).

The resulting stress distribution in the coating region is shown in Fig. 5. It can be noted that at the surface of the zirconia, a compressive residual stress exists after manufacturing. Steady-state

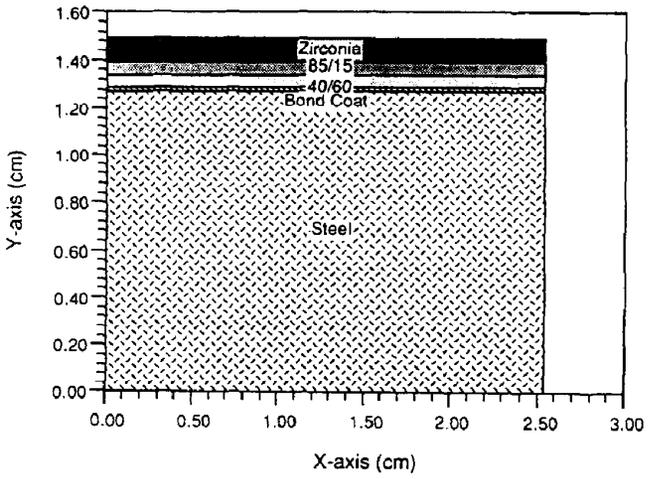

Fig. 1. Specimen configuration.

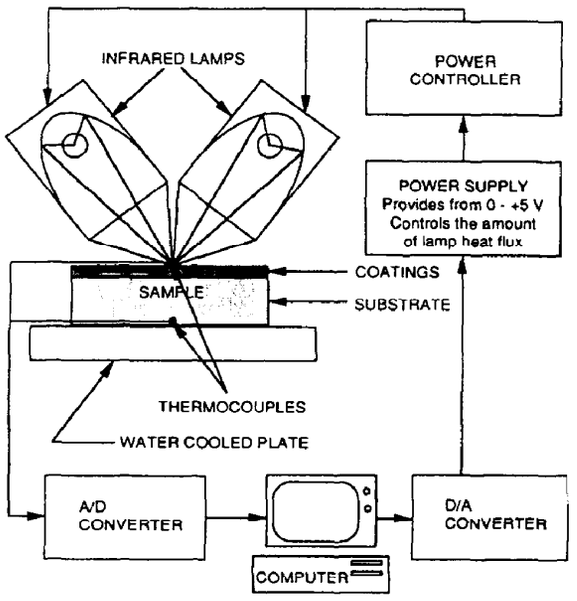

Fig. 2. Schematic of experimental set-up.

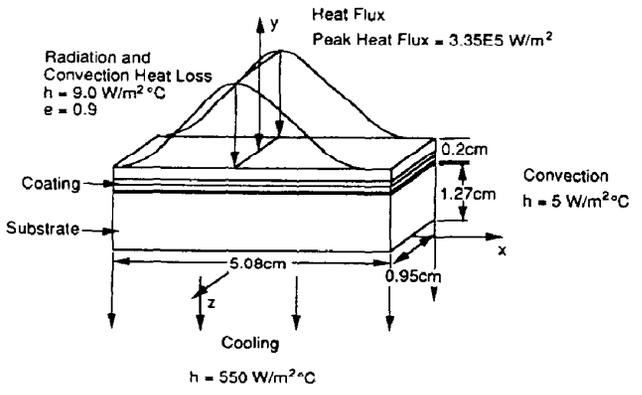

Fig. 3. Experimental boundary conditions.

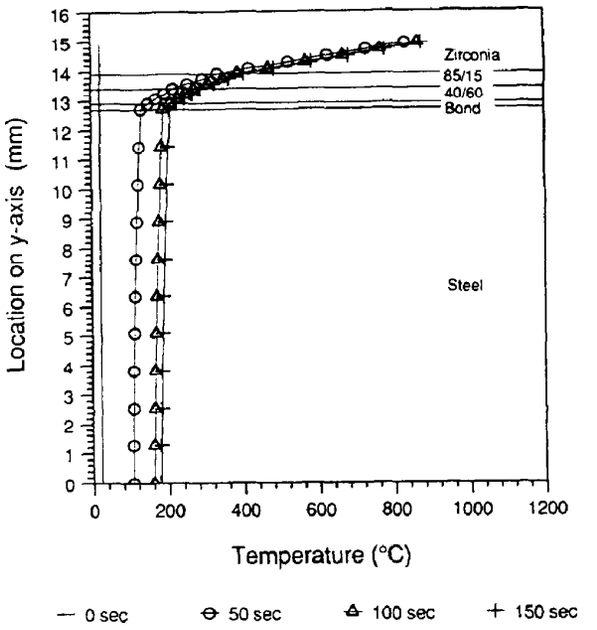

Fig. 4. Temperature distribution in the specimen.

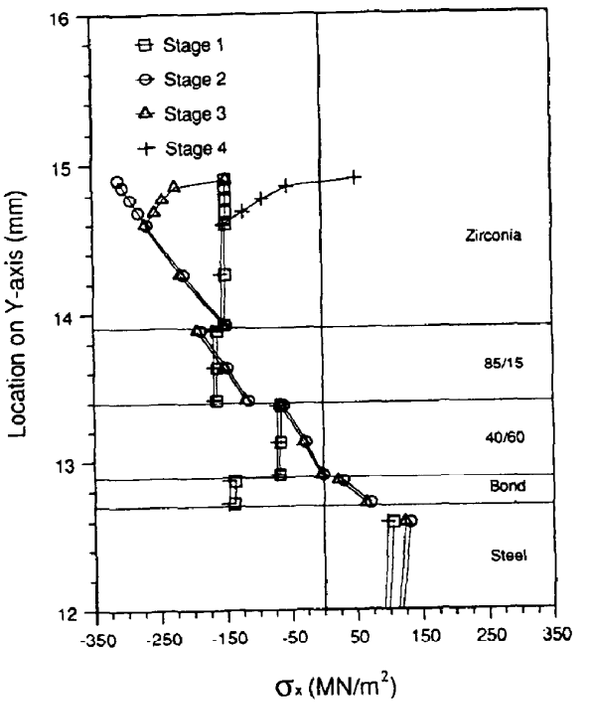

Fig. 5. Stress distribution in the coating layers.

heating of the surface increases the compression which relaxes during the 2 h. Subsequent cooling to room temperature results in a tensile stress which causes the cracks to initiate. This mechanism was also confirmed through measurements of time-dependent strains on the substrate in a different specimen configuration.[6]

3 EFFECT OF COATING ARCHITECTURE ON SURFACE-CRACK INITIATION

The experiments and analysis described above were used to determine the mechanism of crack initiation in zirconia. In order to provide a more systematic study of the effect of changing the architecture to a functionally graded coating, a transient analysis was performed on a simplified model. The surface heat flux was changed to a uniform convective heating condition so that a one-dimensional heat transfer model could be utilized. The stresses were calculated by using a multilayer beam model. The details of this model are presented elsewhere and will not be repeated here.[7]

The maximum transient stresses at the surface of a linearly distributed coating (see Fig. 6) during cooling following stress relaxation are shown in Fig. 7 as a function of coating thickness. It can be noted that a multilayer, graded coating experiences a smaller stress and thus will be more resistant to surface crack initiation.

It can also be noted that as the thickness of the entire coating increases, the stress becomes larger. However, it may be possible to select a multilayer thick coating which will experience a stress similar to a thin single layer coating. Thus, this information allows for a design selection process for a functionally graded coating.

Another parameter which defines the architecture of the coating is the distribution of the layers. This distribution describes the relative thicknesses of the coating layers in relation to their composition. In this analysis, the total coating thickness (t_c) is held constant, while the thicknesses of the individual layers are varied. The distributions are defined by eqns (2) and (3).

$$y_s = \frac{t_c}{n-1}\left(n^{Zf} - 1\right) \tag{2}$$

$$y_s = \frac{nt_c}{n-1}\left(1 - 1n^{Zf}\right) \tag{3}$$

where Z_f is percentage of zirconia, y_s is distance from substrate, n is thickness distribution constant.

These equations allow exponential and logarithmic layer distributions antisymmetric about the

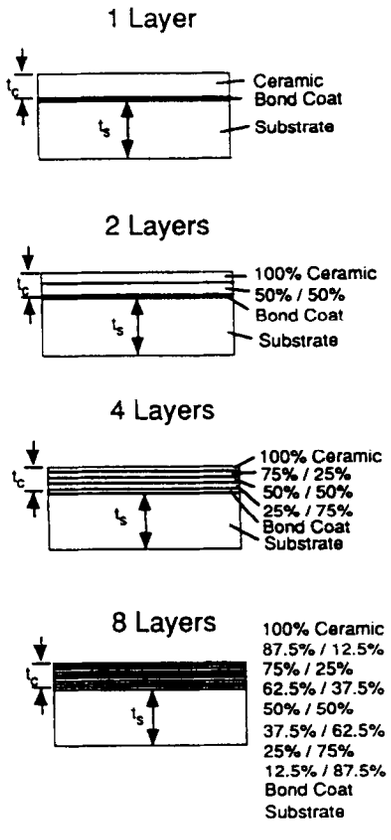

Fig. 6. Architecture for different number of layers.

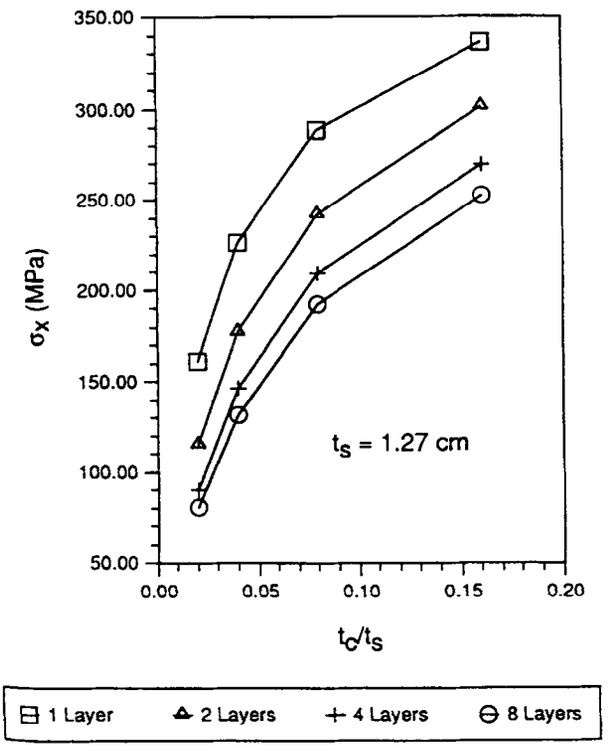

Fig. 7. Maximum surface stress during cooling after 2 h of stress relaxation.

linear distribution for a single value of n. Example distributions are shown in Fig. 8. The resulting coatings that vary exponentially (Exp) and logarithmically (Log) for a 4 layer system are illustrated in Fig. 9. The substrate thickness is 1.27 cm and the coating analysed is 0.2036 cm thick and has four layers.

The steady state surface temperatures vs t_c/t_s for different layer distributions are shown in Fig. 10.

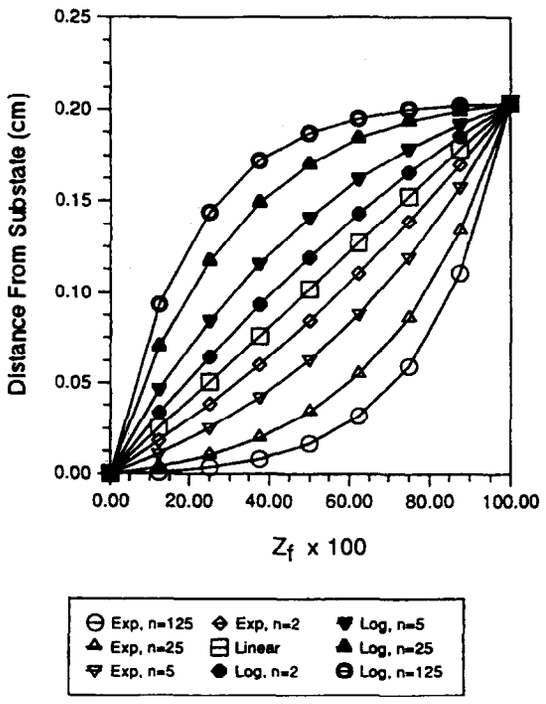

Fig. 8. Different composition distributions.

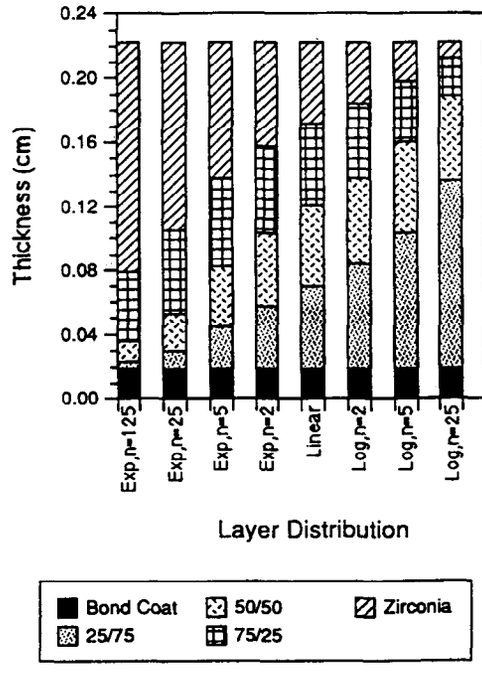

Fig. 9. Representation of composition distribution for 4 layer systems.

The "Log" and "Exp" in the legends of these figures represent logarithmic and exponential. The surface temperature is largest for the exponential distribution with $n = 125$ because this coating has the greatest amount of zirconia of any of the coatings. The coating with the logarithmic distribution

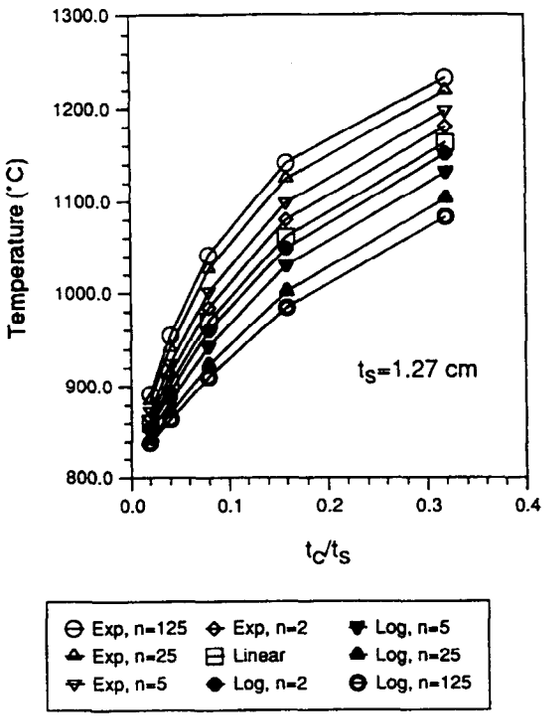

Fig. 10. Steady-state surface temperatures vs coating thickness for a 4 layer system.

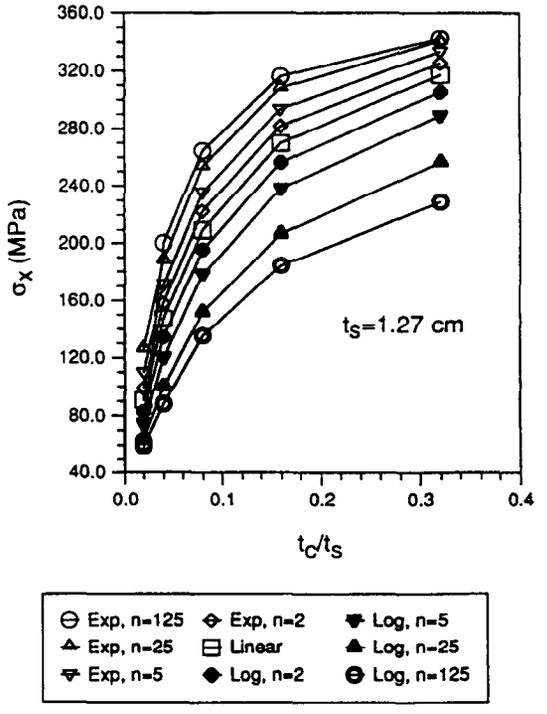

Fig. 11. Maximum surface stress vs coating thickness for a 4 layer system during cooling that follows 2 h of stress relaxation.

($n = 125$) has the least amount of zirconia and thus it has the lowest surface temperature. The thicker coatings all experience a higher surface temperature than the thin coatings.

The maximum stresses during cooling, for each configuration are shown in Fig. 11. The thick ($t_c/t_s = 0.32$) exponential distribution coating with $n = 125$ relaxes more and has a surface stress of 350 MPa during cooling after stress relaxation. The Log, $n = 125$ ($t_c/t_s = 0.02$) coating has the smallest temperature gradient and a maximum surface stress of only 60 MPa. Note that the slope of the maximum surface stress vs t_c/t_s is much steeper for a small thickness ratio. This is because the surface temperature also has a steep slope in this thin coating range. Thus, when the coating is in this thin range, a small change in thickness will have a larger effect on the maximum stress than when the coating is thick.

4 CONCLUSIONS

The results presented here show that surface cracks in multilayer graded ceramic thermal barrier coatings initiate because of tensile stresses which are generated by cooling that follows relaxation of compressive stresses at high temperature.

This failure mechanism is used as the criterion for determining the effect of layer architecture on a functionally graded coating. The results show that a graded system which is relatively thick will have a resistance to thermal crack initiation similar to that of a thinner single layer coating.

The non-linear distribution of the coating architecture with the smallest amount of zirconia results in the smallest surface stresses. However, these results show that a particular design can be selected which will satisfy the stress requirements of a given application.

It is clear that the careful study of failure mechanisms is critical to the successful design of functionally graded ceramic thermal barrier coatings. However, many more issues related to determination of properties, crack initiation mechanisms at interfaces, thermal fatigue behaviour need to be studied in order for these materials to become visible in heat engine applications.

ACKNOWLEDGEMENTS

The support of Cummins Engine Company, Columbus, IN and the National Science Foundation is gratefully acknowledged.

REFERENCES

1. LEVINE, S. R., MILLER, R. & HODGE, P. E., Thermal barrier coatings for heat engine components. *Sampe Quarterly*, **12** (1980) 20–26.
2. MILLER, R. A. & BERNDT, C. C., Performance of thermal barrier coatings in high heat flux environments. *Thin Solid Films*, **119** (1984) 195–202.
3. NESBITT, J. A., Thermal response of various thermal barrier coatings in a high heat flux rocket engine. *Surf. Coat. Technol.*, **43/44** (1990) 458–469.
4. TAKEUCHI, Y. R., Thermal fracture of ceramic thermal barrier coatings. M.S. Thesis, Purdue University, 1991.
5. KOKINI, K. & TAKEUCHI, Y. R., Initiation of surface cracks in multilayer ceramic thermal barrier coatings under thermal loads. *J. Mater. Sci. Engng A*, **189** (1994) 301–309.
6. TAKEUCHI, Y. R. & KOKINI, K., Thermal fracture of multilayer ceramic thermal barrier coatings. *ASME Trans., J. Engng Gas Turb. Power*, **116** (1994) 266–271.
7. CHOULES, B. D. & KOKINI, K., Multilayer ceramic coating architecture against surface thermal fracture. In *Proc. of the Symp. on Ceramic Coatings*, ed. K. Kokini. ASME MD-Vol.44, New York, 1993, pp. 73–86.